

Purified Anthocyanins from Bilberry and Black Currant Attenuate Hepatic Mitochondrial Dysfunction and Steatohepatitis in Mice with Methionine and Choline Deficiency

Xilan Tang,^{†,§} Tianran Shen,[†] Xinwei Jiang,[†] Min Xia,^{†,‡} Xujia Sun,[†] Honghui Guo,^{*,§} and Wenhua Ling^{*,†,‡}

[†]Department of Nutrition, School of Public Health, Sun Yat-Sen University, Guangzhou 510080, P. R. China

[§]Department of Nutrition, Henry Fok School of Food Science and Engineering, Shaoguan University, Shaoguan 512005, P. R. China

[‡]Guangdong Provincial Key Laboratory of Food, Nutrition and Health, Guangzhou 510080, P. R. China

Supporting Information

ABSTRACT: The berries of bilberry and black currant are a rich source of anthocyanins, which are thought to have favorable effects on nonalcoholic steatohepatitis (NASH). This study was designed to examine whether purified anthocyanins from bilberry and black currant are able to limit the disorders related to NASH induced by a methionine-choline-deficient (MCD) diet in mice. The results showed that treatment with anthocyanins not only alleviated inflammation, oxidative stress, steatosis, and even fibrosis but also improved depletion of mitochondrial content and damage of mitochondrial biogenesis and electron transfer chain developed concomitantly in the liver of mice fed the MCD diet. Furthermore, anthocyanins treatment promoted activation of AMP-activated protein kinase (AMPK) and expression of peroxisome proliferator-activated receptor-gamma coactivator-1 α (PGC-1 α). These data provide evidence that anthocyanins possess significant protective effects against NASH and mitochondrial defects in response to a MCD diet, with a mechanism maybe through affecting the AMPK/PGC-1 α signaling pathways.

KEYWORDS: AMP-activated protein kinase, anthocyanin, mitochondrial dysfunction, nonalcoholic fatty liver disease, oxidative stress

■ INTRODUCTION

Nonalcoholic fatty liver disease (NAFLD) is currently the most prevalent chronic liver disease, largely due to the obesity epidemic.¹ It encompasses a spectrum of liver damage ranging from simple steatosis to nonalcoholic steatohepatitis (NASH), an advanced stage of disease comprising progressive steatosis, lobular inflammation, balloon degeneration, and even fibrosis.² The pathogenesis responsible for the development and progression of NASH is comprehensive and remains yet to be fully elucidated. Due to this available treatments remain unsatisfactory.

Hepatocytes are commonly enriched in mitochondria (~1000–2000 mitochondria/hepatocyte), signifying their critical roles within hepatocytes, such as the primary site for energy production and β -oxidation of fatty acids. Previous studies have shown that abnormal morphological changes in mitochondria and reduced mitochondrial DNA (mtDNA) copy number are observed in human subjects and animal models with NASH.^{3,4} In addition, significantly decreased activity of the hepatic mitochondrial respiratory chain (MRC), particularly complex I and IV, was shown in NASH liver samples compared to controls.^{5,6} Moreover, recent evidence has demonstrated impairment of mitochondrial β -oxidation in humans and animals with NASH.^{7,8} These studies provide strong evidence to support the possibility that NAFLD might be a mitochondrial disease. They also support seeking therapies that improve mitochondrial function as a useful strategy for preventing NASH and its complications.

Interestingly, several polyphenolic compounds, such as curcumin,⁹ quercetin,¹⁰ anthocyanins (ACNs)¹¹ and green tea catechins,¹² have been demonstrated to have beneficial effects in NAFLD. Among them, ACNs are of great interest due to their abundance in a wide variety of plant foods and the fact that considerable amounts could be ingested from our plant-based daily diets. Existing in vitro data suggest that ACNs exert antisteatosis effects in hepatocytes by inhibiting lipogenesis and/or promoting fatty acid oxidation.^{13–15} Mirroring the results obtained in vitro, ample evidence from animal models of NAFLD demonstrates that ACNs diminish hepatic lipid accumulation and inflammation.¹⁶ Furthermore, ACNs are thought to promote antioxidant activity and eventually contribute to an overall positive gain in liver function.^{17,18} Despite realizing these benefits, an understanding of the protective role of ACNs and the underlying mechanism of action in the progression of NASH remains unknown and requires further investigation in vivo.

Considering the potential capability of ACNs in NASH and the vital role of mitochondrial dysfunction in the progression of NASH, we set out to determine the influence of purified ACNs from bilberry and black currant on hepatic steatohepatitis and fibrosis as well as mitochondrial content and function in a methionine-choline-deficient (MCD) diet murine model of

Received: October 14, 2014

Revised: December 8, 2014

Accepted: December 23, 2014

Published: December 23, 2014

NASH. The influence of ACNs on related signaling pathways was also investigated.

MATERIALS AND METHODS

Purified Anthocyanins. Purified ACNs were kindly provided by Polyphenol AS (Sandnes, Norway). As mentioned in our previous study,¹⁹ the purified ACNs product consisted of 17 different natural ACNs from bilberry (*Vaccinium myrtillus*) and black currant (*Ribes nigrum*). Cyanidin 3-*O*- β -glucoside and delphinidin 3-*O*- β -glucoside are major components of the ACNs supplement. Detailed components and contents are listed in Supporting Information Table 1.

Reagents and Antibodies. Reagents for immunohistochemistry and immunofluorescence, such as serum blocking solution, hydrogen peroxide, and diaminobenzidine (DAB), were obtained from Zhongshan Jinqiao Biotechnology Co. (Beijing, China). Anti-AMP-activated protein kinase (AMPK) and antiphosphorylated AMP-activated protein kinase (p-AMPK) antibodies were purchased from Cell Signaling Technology Inc. (Danvers, MA, USA). Antibodies for cabamoyl phosphate synthase 1 (CPS-1), alpha smooth muscle actin (α -SMA), peroxisome proliferator-activated receptor- γ coactivator-1 β (PGC-1 β), nicotinamide adenine dinucleotide dehydrogenase (Complex I), and cytochrome *c* oxidase (Complex IV) were purchased from Abcam (Cambridge, UK). Antibodies for peroxisome proliferator-activated receptor- γ coactivator-1 α (PPAR- α), peroxisome proliferator-activated receptor-1 α (PGC-1 α), glyceraldehyde 3-phosphate dehydrogenase (GAPDH), and all secondary antibodies were obtained from Santa Cruz Biotechnology (Santa Cruz, CA, USA). Fluorescent probe dihydroethidium (DHE) was purchased from Calbiochem (San Diego, CA, USA). All other reagents and kits were obtained from Sigma-Aldrich (St. Louis, MO, USA) and Invitrogen (Carlsbad, CA, USA) unless otherwise noted.

Animals and Diets. All animal procedures were approved by the Animal Care and Protection Committee of Sun Yat-Sen University (2013-10). Six-week-old male C57BL/6J mice purchased from the Experimental Animal Center of Sun Yat-Sen University (Guangzhou, China) were housed in standard cages within a room with a constant temperature and humidity, under a 12-h light/dark cycle, with free access to food and water. After 2-week adaptation, all mice were body-weight matched and randomly divided into three groups ($n = 8$ per group): (1) control group, mice were fed a control chow diet; (2) MCD group, mice were fed with a diet deficient in methionine and choline; (3) MCD + ACNs group, mice were fed with the MCD diet with addition of 1 g of purified ACNs per kilogram food. Both the control chow diet and MCD diet were purchased from Research Diets Inc. (New Brunswick, NJ, USA). The control diet was identical to the MCD diet but supplemented with D,L-methionine (3 g/kg) and choline chloride (2 g/kg). Food intake was measured every other day, and body weight was measured weekly.

Biochemical Analyses. At the end of the experiment, all mice were euthanized with sodium pentobarbital (50 mg/kg body weight) and sacrificed after overnight starvation. The serum and liver samples of each mouse were collected and stored at -80°C for further analysis.

Serum alanine aminotransferase (ALT) and aspartate aminotransferase (AST) were detected using commercial kits from Jiancheng Bioengineering Institute (Nanjing, China) according to the manufacturer's instructions. Serum triglyceride (TG), total cholesterol (TC), and hepatic TG/TC contents were determined using commercial detection kits (Applygen Technologies Inc., Beijing, China) according to manufacturer's protocols.

Histological Assessment. The liver samples were fixed in 10% phosphate-buffered formalin, embedded in paraffin, cut in 5 μm thickness, and applied to slides. The sections were stained with hematoxylin and eosin (H&E) and Sirius Red for histological analysis (NAFLD activity scoring (NAS) and collagen) under light microscopy (Leica, Bensheim, Germany). The Pathology Committee of the NASH Clinical Research Network²⁰ provided guidance and recommendations for the NAS study by semiquantitatively evaluating the following histological features: steatosis (<5% = 0; 5–33% = 1; 33–66% = 2; >66% = 3); lobular inflammation (none = 0; <2 foci = 1; 2–4 foci = 2; >4

foci = 3); and hepatocellular ballooning (none = 0; few = 1; prominent = 2). All features were scored blindly based on at least 5 samples per group and 10 fields of vision in each sample. Fresh liver tissue was embedded in Tissue Tek OCT, rapidly frozen in liquid nitrogen, and then stored at -80°C for preparation of frozen sections (5 μm), which were used for staining with Oil Red O and immunofluorescence staining.

Immunohistochemistry and Immunofluorescence. The procedures for immunohistochemistry and immunofluorescence assays were performed as previously described.²¹ Briefly, slides were incubated in serum blocking solution for 30 min and incubated overnight with either α -SMA or CPS-1 primary antibody. Then HRP-labeled or fluorescent secondary antibodies were used for immunohistochemistry (α -SMA) and immunofluorescence (CPS-1) analysis, respectively. DAB was applied for immunohistochemistry, and the samples were observed under light microscopy (Leica, Bensheim, Germany). DAPI (Roche, Germany) was utilized for immunofluorescence nuclear staining, and the samples were observed under an Inverted Fluorescence Microscopy (Nikon Eclipse Ti-E, Tokyo, Japan). The fluorescent intensity was analyzed using ImageJ software (Research Services Branch of the NIH, Bethesda, MD).

Western Blot. Liver tissues were homogenized, and 30 μg of total protein lysate were loaded onto 8–15% SDS polyacrylamide gels. After 90 min of electrophoresis, the proteins were transferred onto a polyvinylidene difluoride membrane in ice for 1–2 h. The membrane was blocked with 5% (w/v) bovine serum albumin dissolved in trihydroxymethyl aminomethane buffer salt containing 0.05% (v/v) Tween-20 (TBST). The membrane was then incubated at 4°C overnight with primary antibodies for AMPK, p-AMPK, CPS-1, PGC-1 α , PGC-1 β , PPAR- α , Complex I, or Complex IV, followed by incubation with secondary antibodies conjugated with horseradish peroxidase for 2 h at room temperature. Signals were detected by enhanced chemiluminescence reagent (Thermo Fisher Scientific, Waltham, MA, USA). GAPDH was used for normalization. The density of the specific bands was quantified using ImageJ software.

Mitochondrial DNA Quantification. Total DNA was extracted from livers using a DNeasy Blood & Tissue Kit (Qiagen, Dusseldorf, Germany), and real-time PCR was performed using gene-specific primers amplifying mitochondrial DNA (mtDNA) and nuclear DNA (nDNA). The relative values of mtDNA content and nDNA content were used to assess mitochondrial copy numbers. The primer sequences are listed in Supporting Information Table 2.

RNA Extraction and Quantitative RT-PCR. Total RNA (1 μg) was extracted from liver tissues using Trizol reagent and transcribed into cDNA using the PrimeScript RT reagent kit (TaKaRa, Tokyo, Japan) according to the manufacturer's recommendations. Quantitative PCR was performed using a real-time PCR system (Applied Biosystems, Foster City, CA, USA), and reactions were performed using SYBR Green Master Mix (TaKaRa, Tokyo, Japan) with gene-specific primers. Each sample was normalized to β -actin, and the fold change in expression of each target gene relative to β -actin was assessed via the comparative CT ($2^{-\Delta\Delta\text{CT}}$) method. Primer sequences are listed in Supporting Information Table 3.

Detection of Hepatic Oxidative Stress. The total reactive oxygen species (ROS) levels in the liver tissues were detected using the fluorescent probe DHE. Briefly, frozen liver sections were incubated in DHE (10 μM) for 30 min in a dark and humidified chamber at 37°C . DHE is oxidized by superoxide to ethidium bromide, binds to the DNA, and emits red fluorescence,²² which was detected using inverted fluorescence microscopy. In addition, liver tissue homogenates were prepared to measure hepatic malondialdehyde (MDA) by following the commercial kit's instructions (Beyotime, Shanghai, China). The MDA concentrations were normalized by protein contents.

Statistical Analysis. All results were expressed as mean \pm standard deviation (SD) and statistically analyzed with SPSS 16.0 for Windows (SPSS Inc., Chicago, IL, USA). Comparisons between all groups were evaluated using one-way analysis of variance (ANOVA). Differences were considered significant at $P < 0.05$.

RESULTS

Effects of ACNs on Animal Characteristics. As shown in Table 1, the initial body weight among the 3 groups showed little

Table 1. Animal Characteristics and Serum Liver Enzymes of Mice in Different Study Groups^a

	control	MCD	MCD + ACNs
initial body weight (g)	25.12 ± 1.30	25.09 ± 1.26	25.35 ± 1.20
final body weight (g)	27.39 ± 2.74	16.93 ± 0.73*	17.19 ± 0.42*
liver weight (g)	0.89 ± 0.13	0.54 ± 0.06*	0.56 ± 0.10*
liver to body weight ratio (%)	3.53 ± 0.62	3.20 ± 0.20	3.40 ± 0.34
serum ALT level (U/L)	6.03 ± 1.68	79.08 ± 36.54*	58.65 ± 25.03*/#
serum AST level (U/L)	23.43 ± 1.66	49.48 ± 3.17*	40.26 ± 2.07*/#

^aAll values are mean ± SD, *n* = 8. Statistical analysis of the data for multiple comparisons was performed by ANOVA. **P* < 0.05 versus the control group; #*P* < 0.05 versus the MCD group.

deviation (*P* > 0.05). After 4 weeks, the MCD mice with or without ACNs treatment displayed a significant reduction in body weight (~50%). Moreover, 1-fold increase in serum AST and more than 10-fold increase in serum ALT were observed in mice fed the MCD diet. Though ACNs did not attenuate the reduction of body weight induced by the MCD diet, their addition effectively decreased serum ALT and AST levels (*P* < 0.05). No significant changes in daily food intake among the 3 groups during the experimental period were observed (data not shown).

Effects of ACNs on Lipid Accumulation. The histological features of Oil Red O staining illustrated a massive accumulation of neutral lipid droplets within the hepatocytes of MCD group, whereas only small lipid droplets were observed in mice treated with ACNs (Figure 1A). Quantitative determination of hepatic TG content further confirmed that a large quantity of TG accumulated in the livers of mice fed the MCD diet, which was significantly decreased by ACNs supplementation (*P* < 0.05) (Figure 1B). Conversely, the serum TG levels in both MCD diet group and MCD + ACNs group declined sharply compared with the control group, while were slightly up-regulated by ACNs though without significance compared with the MCD group (*P* > 0.05) (Figure 1C). This interesting phenomenon probably was

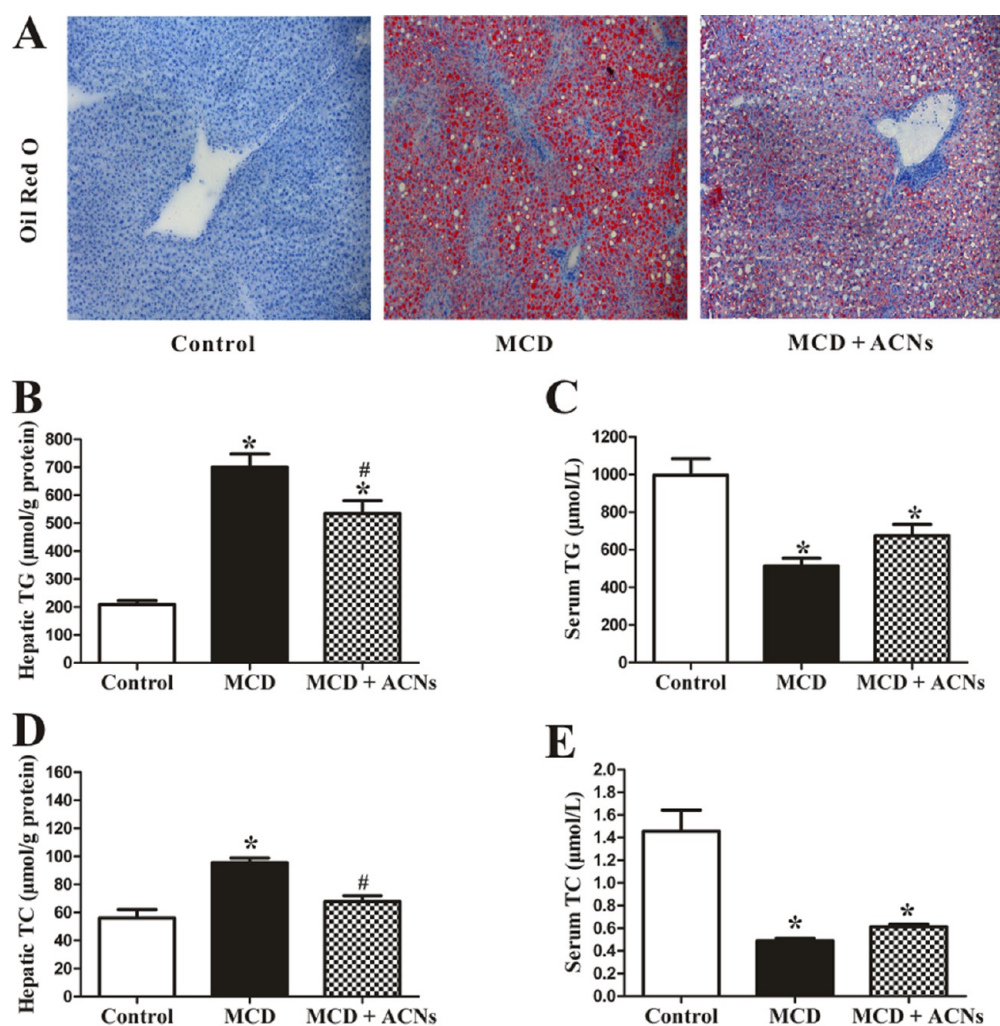


Figure 1. ACNs decreased lipid accumulation in mice fed the MCD diet. (A) Frozen sections (5 μm thick) were stained with Oil Red O, which marked neutral lipid. Representative micrographs (200× magnification) are shown. (B–E) TG and TC levels were measured from all frozen liver specimens and serum. Values are expressed as mean ± SD, *n* = 8. **P* < 0.05 versus the control group; #*P* < 0.05 versus the MCD group.

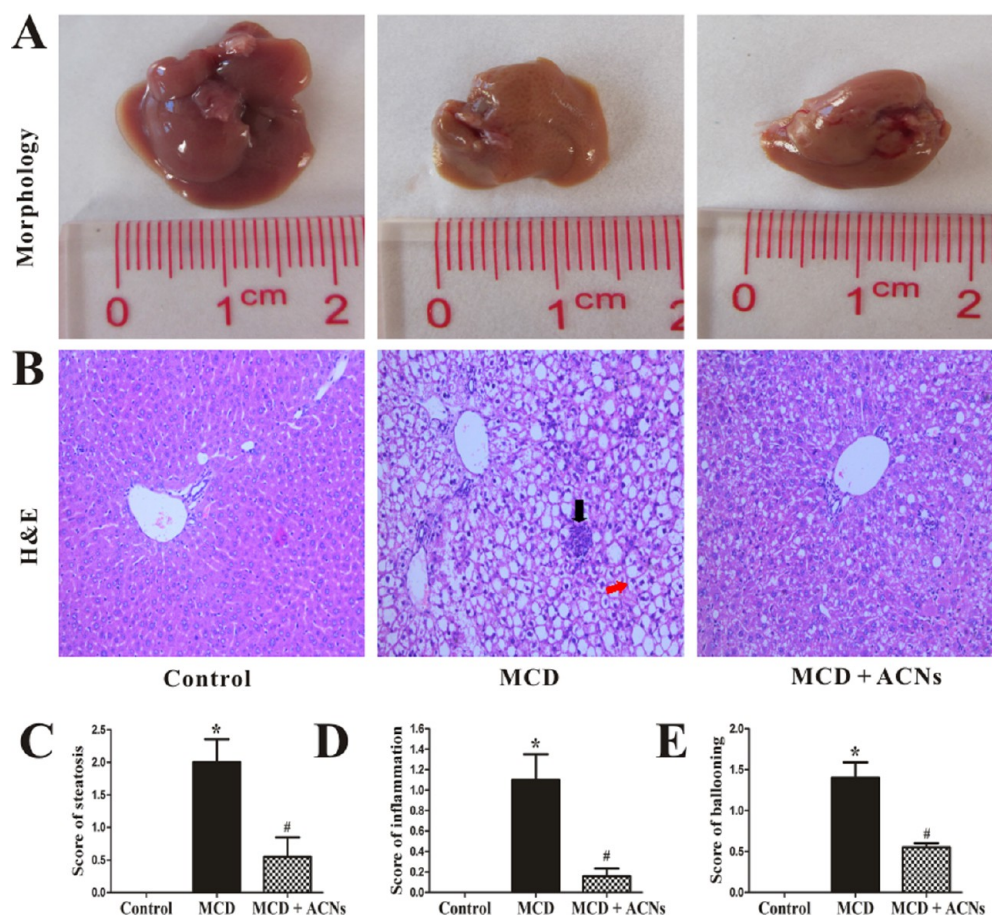


Figure 2. ACNs ameliorated steatohepatitis induced by the MCD diet. (A) Representative gross morphology images are shown. (B) Hepatic histological analysis of H&E staining (200 \times magnification). Inflammatory infiltration (black arrow) and hepatocyte ballooning (red arrow) were observed in liver sections from the MCD group which were improved in the ACNs-treated group. (C–E) Histological NAS scores of liver tissues. Values are expressed as mean \pm SD, $n = 8$. * $P < 0.05$ versus the control group; # $P < 0.05$ versus the MCD group.

caused by hepatic TG potentially releasing into serum. Similarly, accumulation of hepatic TC was effectively alleviated by ACNs ($P < 0.05$) (Figure 1D). The serum TC levels in the MCD + ACNs group showed an increasing trend but no significant differences compared to the MCD diet only group (Figure 1E).

Amelioration of Steatohepatitis by ACNs. The gross morphology of the livers in the control group displayed red and smooth tissue surface. After 4 weeks feeding with MCD diet, the gross morphology of livers had an obvious increase in tawny and brittle appearance, which was improved greatly by ACNs treatment (Figure 2A). The NAS calculation system was applied to semiquantitatively evaluate the steatosis, inflammation, and ballooning. Indeed, the histological analysis of H&E staining indicated significant microvesicular steatosis, inflammatory cell infiltration, and hepatocyte ballooning in the MCD diet group. However, livers of the ACNs-treated group exhibited only mild hepatic steatosis and effectively ameliorated inflammatory infiltration with reduction by 50% in hepatocyte ballooning compared to the MCD diet only group (Figure 2B–E).

Inhibition of Liver Fibrosis by ACNs. To assess the effect of ACNs on hepatic fibrosis, we carried out a Sirius Red staining of collagen in liver sections. A substantial increase in collagen deposition was observed in the MCD group compared with the control group. However, an obvious decrease in the stained area percentage was observed in the MCD + ACNs group (Figure 3A). Activation of hepatic stellate cells (HSCs), the major effectors in collagen production during hepatic fibrogenesis, is

another indicator of fibrogenesis. To further evaluate HSCs activation, immunohistochemical staining of α -SMA was performed. As displayed in Figure 3B, the data indicated that ACNs treatment reduced the expression of α -SMA, suggestive of inhibition of HSCs activation. Besides, both relative mRNA expression of collagen I and α -SMA confirmed that ACNs played a suppressive effect on fibrosis in NASH (Figure 3C and 3D).

Decrease of Oxidative Damage by ACNs. Mitochondria are the major sites for ROS production. Quantitative evaluation of hepatic ROS is also an indicator of mitochondrial impairment. In our present study, the 4-week MCD diet up-regulated ROS levels of liver tissues by approximately 6-fold compared with the control diet, and we unearthed that ACNs were able to significantly subdue ROS production induced by the MCD diet (Figure 4A and 4B). In addition, hepatic malondialdehyde (MDA) content, a widely used marker of oxidative stress, was increased by nearly 4-fold in the MCD group but only slightly increased in ACNs-treated mice (Figure 4C). The results of hepatic ROS and MDA levels clarified that ACNs played a suppressive effect on oxidative damage in NASH.

Attenuation of Reduced Mitochondrial Content and Function by ACNs. One of the common mitochondrial defects observed in NASH is depletion of mitochondrial DNA (mtDNA).⁴ In our study, we first investigated the protective effect of ACNs on mtDNA. As shown in Figure 5A, mtDNA indeed displayed an apparent decrease in the MCD group, which was slightly improved through administration of ACNs ($P <$

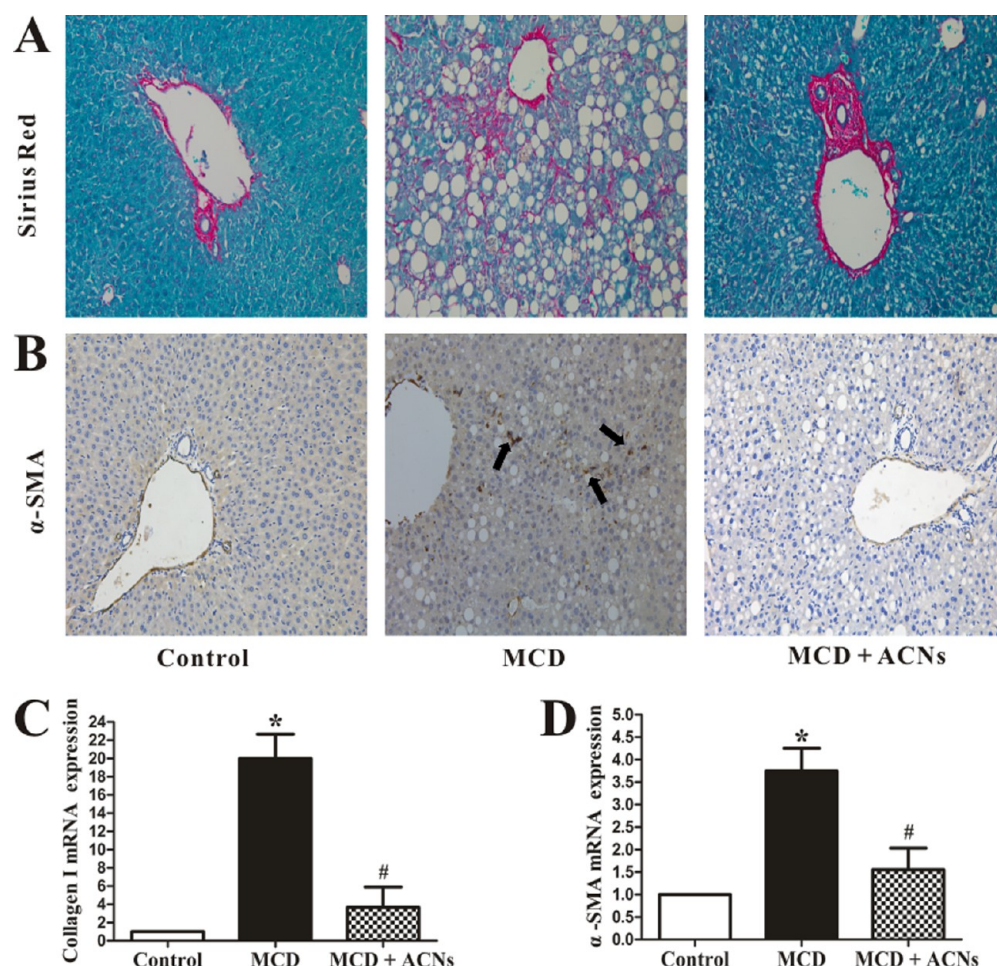


Figure 3. ACNs played an inhibitory role in progression of fibrosis in mice fed an MCD diet. (A) Paraffin-embedded liver specimens were stained with Sirius Red and observed by light microscopy. (B) Paraffin sections were immunoassayed for fibrosis markers, α -SMA (black arrows), to assess hepatic stellate cells activation. Representative photographs (200 \times magnification) are shown. (C and D) Total RNA was isolated from the livers, and genes expression of collagen I and α -SMA were subjected to RT-PCR analysis; the control group was set to be 1. Values are expressed as mean \pm SD, $n = 8$. * $P < 0.05$ versus the control group; # $P < 0.05$ versus the MCD group.

0.05), though it was still lower than the number observed in the control group. Moreover, CPS-1, a hepatic mitochondrial membrane specific marker and reflection of mitochondrial number and function in liver, declined in NASH but was significantly up-regulated by treatment of ACNs (Figure 5B–5D).

Enhancement of Mitochondrial Biogenesis by ACNs.

To investigate whether ACNs are capable of increasing mitochondrial biogenesis, we determined the relative mRNA expression of peroxisome proliferator-activated receptor- γ coactivator-1 α (PGC-1 α) and β (PGC-1 β), nuclear respiratory factor-1 (NRF-1) and 2 (NRF-2), and mitochondrial transcription factor A (Tfam) (pivotal regulators of mitochondrial biogenesis). As displayed in Figure 6A and B, PGC-1 α dropped in NASH ($P < 0.05$) but exhibited sharply increased expression after ACNs intervention, whereas PGC-1 β was unaffected by either MCD diet or ACNs treatment. In addition, there was almost 50% reduction in PGC-1 α -target genes NRF-1, NRF-2, and TFAM following a MCD diet, while the reduction was effectively suppressed with treatment of ACNs. Likewise, immunoblotting analysis revealed that ACNs reversed the reduction of protein abundance of PGC-1 α induced by the MCD diet, while no significant difference in PGC-1 β expression was observed among the three groups (Figure 6C). Together,

these results indicate that ACNs may induce mitochondrial biogenesis through PGC-1 α pathway.

Our previous research has demonstrated activation of AMPK by ACNs in hepatocytes,¹⁴ which could result in phosphorylation of the transcriptional coactivator PGC-1 α , thus leading to increased mitochondrial biogenesis.^{23,24} Then, we determined the protein levels of p-AMPK and total AMPK and discovered an over 50% decrease in p-AMPK in the liver of NASH mice, which was rescued by ACNs with no change of total AMPK (Figure 6C).

Amelioration of Mitochondrial Electron Transfer Chain (ETC) Defects by ACNs. Mitochondrial ETC is constituted of four respiratory complexes (complexes I–IV).²⁵ To confirm the alteration of mitochondrial ETC and effects of ACNs on it at a functional level, the protein expression of two major sites of electron input into the electron transport system (complex I and IV) in total liver lysates was examined (Figure 6D). The mice fed the MCD diet had mitochondrial ETC defects, as shown by conspicuously diminished protein expression of mitochondrial complexes I and V, especially complex IV (approximately 4-fold). As expected, dietary ACNs intervention successfully intensified protein expression of mitochondrial complexes I and V, reflecting improvement of mitochondrial oxidative phosphorylation and enhancement of mitochondrial biogenesis and function.

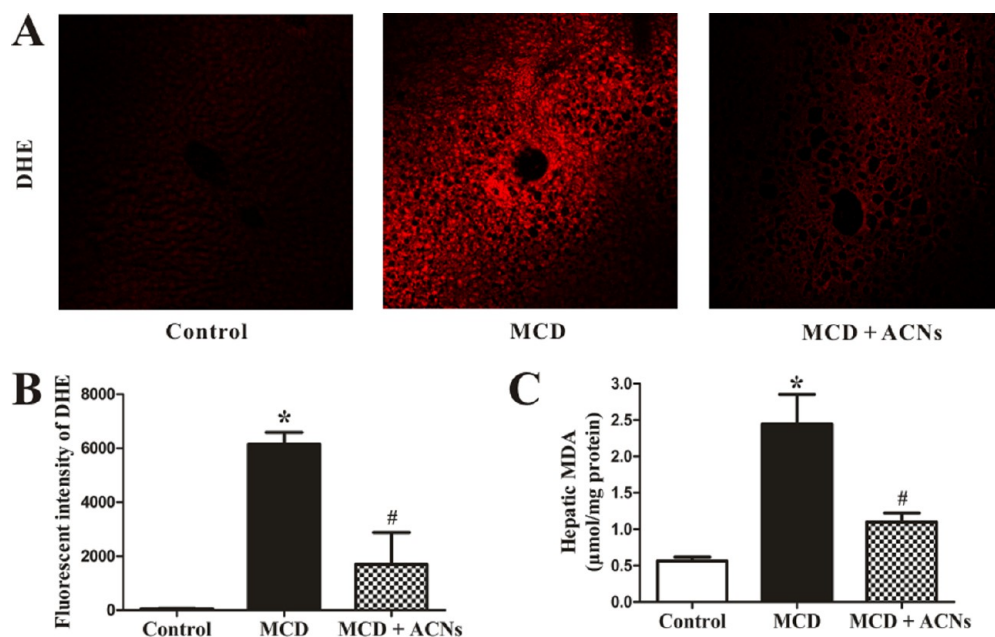


Figure 4. ACNs decreased oxidative damage in NASH. (A) Frozen sections of livers were stained with fluorescent probe DHE, showing red fluorescence in regions of ROS production. Representative fluorescence micrographs (200× magnification) are shown. (B) Fluorescent densitometry of DHE staining was quantified by ImageJ software. (C) MDA content in livers. Values are expressed as mean \pm SD, $n = 8$. * $P < 0.05$ versus the control group; # $P < 0.05$ versus the MCD group.

Improvement of Mitochondrial β -Oxidation by ACNs.

Impairment of mitochondrial oxidative phosphorylation is often followed by inhibition of mitochondrial fatty acid β -oxidation. In the present study, we indeed discovered that both protein and mRNA expression of peroxisome proliferator-activated receptor- α (PPAR- α) were nearly halved in NASH but successfully restored by ACNs intervention (Figure 6C and E). PPAR- α is one of a superfamily of nuclear hormone receptors and able to transcriptionally up-regulate nuclear genes encoding mitochondrial fatty acid oxidation enzymes.²⁶ We then determined gene expression levels of carnitine palmitoyltransferase 1 (CPT-1) and medium chain acyl CoA dehydrogenase (MCAD), two rate-limiting enzymes of fatty acids β -oxidation. As illustrated in Figure 6E, relative mRNA expression of CPT-1 and MCAD dropped significantly in NASH ($P < 0.05$); however, both were augmented with administration of ACNs. These were accompanied by no distinction of fatty acid synthesis (FAS) between the groups. Thus, ACNs seemed to be able to stimulate hepatic lipid oxidation, leading to reduction of TG accumulation within hepatocytes.

DISCUSSION

Previously, we and others have shown that ACNs have hepatoprotective activities in obese and diabetic rodents.^{16,27} In the present study, we demonstrated that purified ACNs from bilberry and black currant were capable of ameliorating hepatic steatosis, inflammation, oxidative stress, as well as signs of fibrosis and improving depletion of mitochondrial content and damage of mitochondrial biogenesis, ETC, as well as β -oxidation. To our knowledge, this work provides the first evidence that ACNs, the soluble flavonoids, alleviate complications of NASH and improve degeneration of mitochondrial function in mice fed a MCD diet.

Much research verifies that abnormalities in the number and quality of mitochondria are frequently observed in NASH and involved in its pathogenesis. These mitochondrial abnormalities include ultrastructural lesions, depletion of mtDNA, reduction of

respiratory chain activity, impairment of mitochondrial β -oxidation, and induction of uncoupling and apoptosis.²⁸ As expected, our MCD diet-induced NASH model displayed a reduction in mitochondrial content as well as impairment of mitochondrial biogenesis, ETC activity, and β -oxidation function.

In our study, we discovered that dietary supplement of ACNs could ameliorate the depletion of mtDNA and decrease expression of CPS-1 (Figure 5). Mitochondrial DNA represents mitochondrial self-replication and is involved in mitochondrial biogenesis.²⁴ It is also crucial for mitochondrial oxidative phosphorylation, encoding 13 MRC polypeptides that embed within complexes I, III, IV, and V, and further for β -oxidation.²⁹ CPS-1, a hepatic mitochondrial membrane-specific marker, qualitatively reflects hepatic mitochondrial content and function in the liver and is a comprehensive marker of mitochondrial damage.³⁰ It could be concluded from our work that dietary ACNs mitigate the depletion of mitochondrial content and dysfunction in NASH.

Mitochondrial biogenesis plays a critical role in maintaining the dynamic equilibrium of proliferation and degradation of mitochondria in hepatocytes.³¹ Activation of mitochondrial biogenesis is mainly reflected by the activation of NRF-1 and NRF-2, which conversely regulates the expression of Tfam, a protein essential for transcription, replication, and maintenance of the mtDNA. In our study, the mRNA expression of NRF-1, NRF-2, and Tfam was significantly decreased in mice fed the MCD diet, indicating damage to mitochondrial biogenesis. This effect was evidently ameliorated by administration of ACNs, especially with respect to NRF-2 and Tfam (Figure 6B). These data suggest that ACNs stimulate mitochondrial biogenesis in NASH.

As major sites for cellular respiration, mitochondria play a vital role in maintaining energy metabolism and function of hepatocytes, which includes the citric acid cycle and oxidative phosphorylation process. The oxidative phosphorylation process

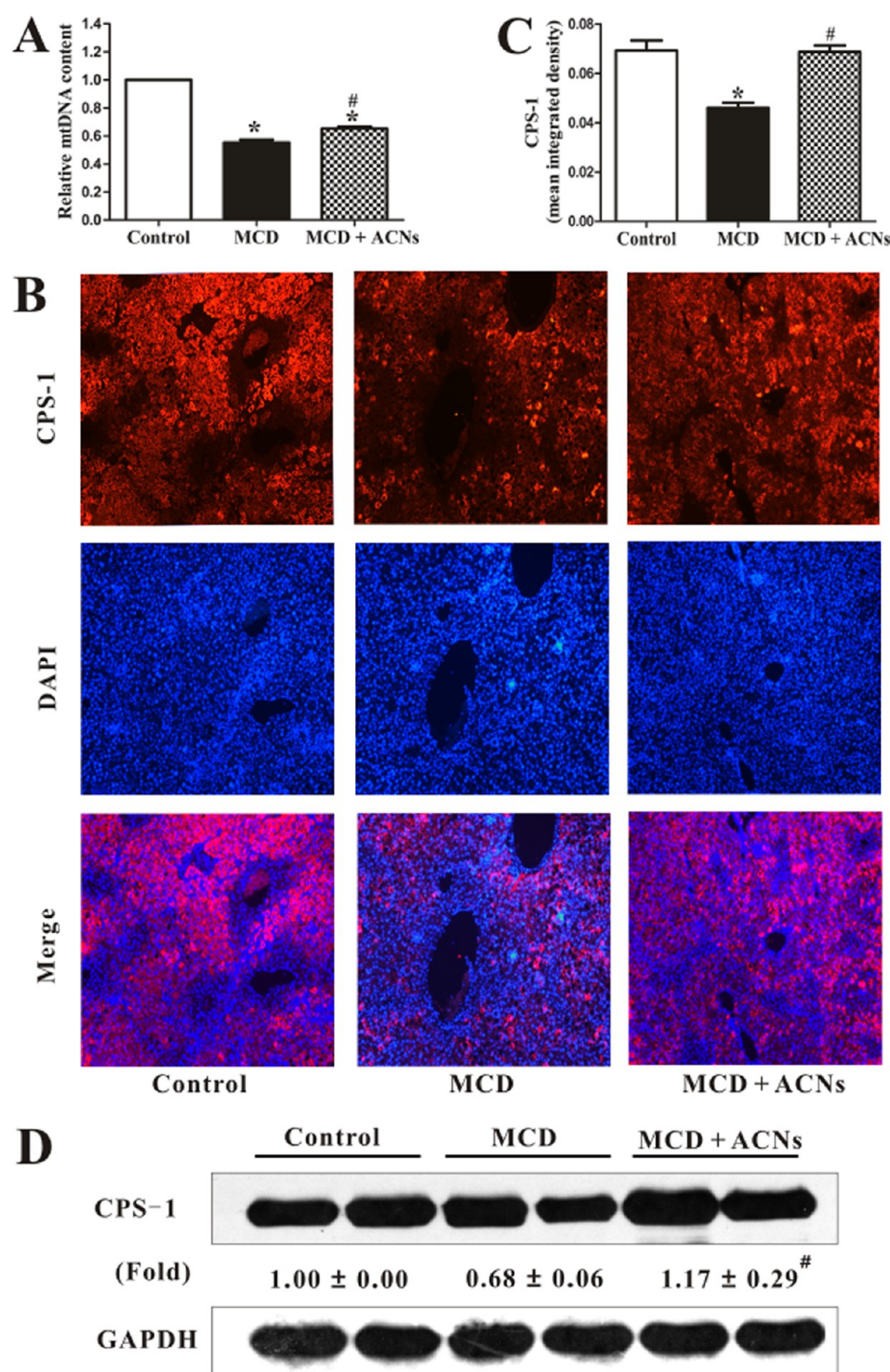


Figure 5. ACNs attenuated reduction of mitochondrial content and function in NASH. (A) Mitochondrial genome copy number was shown as the ratio of mtDNA to nDNA from purified liver DNA, which was determined by quantitative real-time PCR. The control group was set to be 1. (B) Representative immunofluorescent photomicrographs (200× magnification) for mitochondrial marker CPS-1 (red fluorescence) showed granular staining patterns in liver frozen sections. (C) Fluorescent staining of CPS-1 per field was quantified by ImageJ software and reported as mean integrated density. (D) Western blot analysis was performed to semiquantitatively assess expression levels of CPS-1 from liver homogenates. The control group was set to be 1. Values are expressed as mean ± SD, $n = 8$. * $P < 0.05$ versus the control group; [#] $P < 0.05$ versus the MCD group.

of ETC is located on the inner membrane of mitochondrion and consisted of four large transmembrane protein complexes (mitochondrial respiratory complexes I–IV).²⁵ Complexes I and IV are two important and major protein complexes of the electron transfer chain among the four. Via determination of the

two representative protein complexes, we ascertained that ETC defects happened in mice fed the MCD diet which, however, were visibly alleviated by ACNs administration (Figure 6D).

One of the most common hepatic cell injuries is the result of accumulation of various lipids, which further contributes to

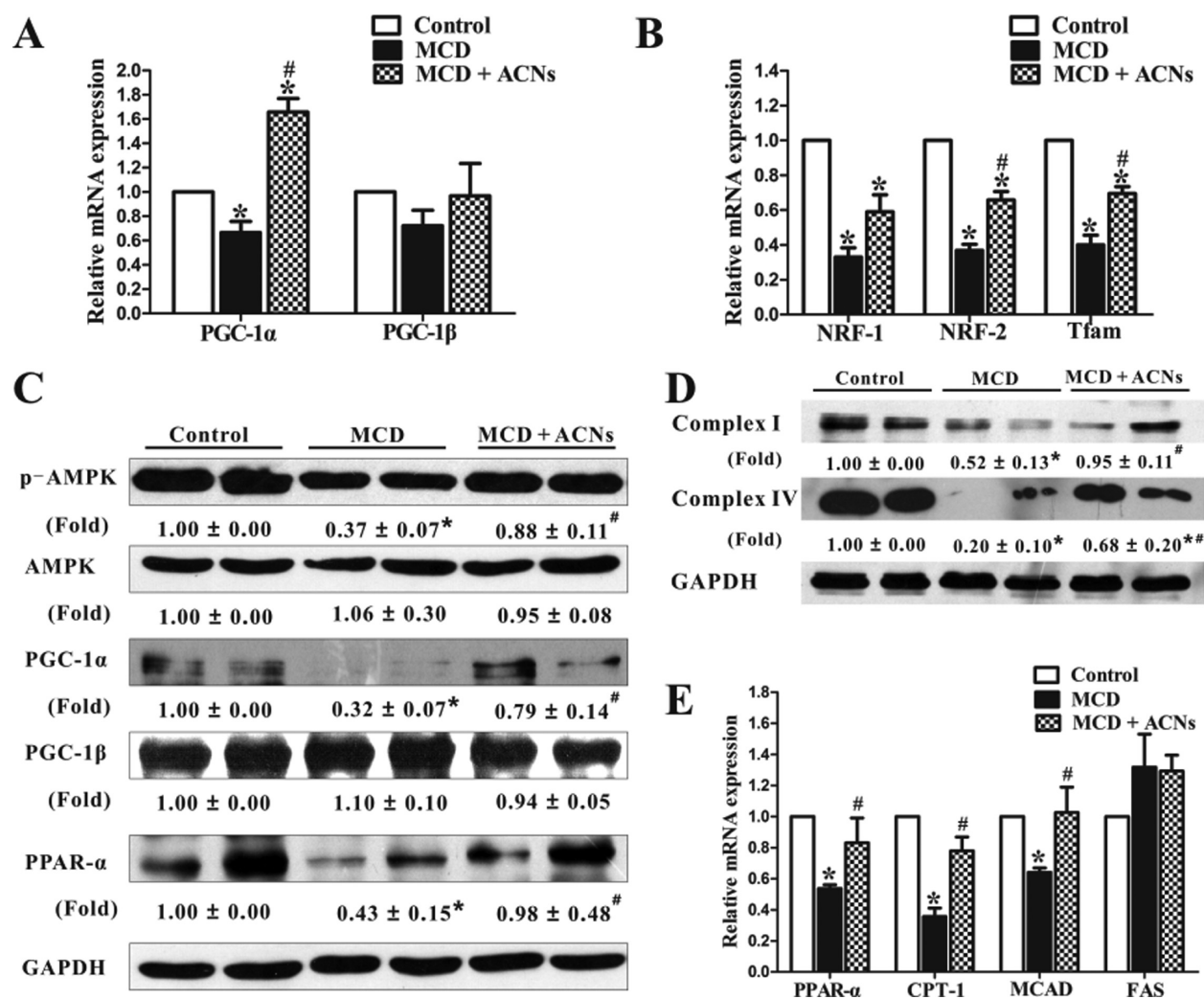


Figure 6. ACNs stimulated mitochondrial biogenesis and improved mitochondrial ETC defects as well as enhanced mitochondrial β -oxidation in NASH. (A and B) Real-time PCR was applied to measure mRNA expression of PGC-1 α and PGC-1 β (A) and genes related to mitochondrial biogenesis (NRF-1, NRF-2 and Tfam) (B). (C) Protein expression of p-AMPK, total AMPK, PGC-1 α , PGC-1 β , and PPAR- α in livers was measured by Western blot, quantified using densitometry, and normalized by GAPDH content. (D) Protein levels of complexes I and IV were examined by Western blot. (E) Genes related to fatty acid oxidation (CPT-1, MCAD, and PPAR- α) and lipogenesis (FAS) were subjected to RT-PCR analysis. The control group was set to be 1. Results are expressed as mean \pm SD, $n = 6-8$. * $P < 0.05$ versus the control group; # $P < 0.05$ versus the MCD group.

development and progression of fatty liver. The main mechanisms are as follows: increased fatty acid uptake and de novo hepatic lipogenesis, decreased fatty acid β -oxidation and hepatic very low density lipoprotein-triglyceride (VLDL) secretion. One of the mechanisms of NASH induced by the MCD diet is decreased VLDL assembly and secretion, contributing to disturbance in phosphatidylcholine synthesis that is caused by deficiencies in methionine and choline.³² In our study, we also observed that this model was accompanied by impairment of mitochondrial β -oxidation, manifested by a decrease in gene or protein expression of PPAR- α , CPT-1, and MCAD (Figure 6C and 6E), which consequently cooperated with decreased VLDL to result in the reduction of lipid clearance. Our data show that ACNs treatment significantly up-regulated protein expression of PPAR- α and gene expression of PPAR- α , CPT-1, and MCAD (Figure 6E). PPAR- α is predominantly expressed in the liver where it transcriptionally up-regulates nuclear genes encoding mitochondrial fatty acid oxidation enzymes CPT-1 and MCAD.²⁶ CPT-1 locates on the outer mitochondrial membrane and is a key rate-limiting enzyme of

long-chain fatty acid β -oxidation, while MCAD is a key enzyme in the first step of medium-chain fatty acid β -oxidation. We conclude that ACNs can improve impairment of mitochondrial β -oxidation in NASH induced by the MCD diet, which further counteracts hepatocyte injury resulting from lipid accumulation by promoting TG clearance.

In line with existing research illustrating that ACNs are able to activate protein expression of AMPK in vitro¹⁴ and in vivo,¹⁶ we also found that ACNs could attenuate the reduction of p-AMPK expression induced by the MCD diet (but not total AMPK; Figure 6C). Moreover, emerging evidence showed that the activation of AMPK leads to increased expression of the downstream molecule PGC-1 α ,³³ which was demonstrated to be a potent stimulator of mitochondrial biogenesis in liver, heart, and skeletal muscle by contributing to activation of NRF-1, NRF-2, and Tfam.³⁴ In the present study, we showed that protein and gene expression of PGC-1 α and its target genes were up-regulated by ACNs, which subsequently potentiated mitochondrial biogenesis. These data suggest that the improvement of mitochondrial dysfunction induced by ACNs treatment is

attributed to increased phosphorylation of AMPK, which subsequently increased expression of PGC-1 α , rather than PGC-1 β (Figure 6A and 6C).

In summary, our study shows that ACNs ameliorate liver disease in steatohepatitis progression and improve mitochondrial defects. Our previous study also showed that anthocyanin cyanidin 3-O- β -glucoside could notably improve mitochondrial function in high glucose-stressed hepatocytes.³⁵ Considering previous studies reporting that mitochondrial dysfunction takes precedence over insulin resistance and hepatic steatosis and leads to the natural history of NAFLD^{30,36} and combining with our own results, we venture to conclude that administration of ACNs attenuated NASH due to the improvement of mitochondrial dysfunction in mice fed a MCD diet. The possible mechanism may involve activation of AMPK/PGC-1 α signaling axis by ACNs, which subsequently contributes to improvement of depletion of mitochondrial mtDNA and mitochondrial biogenesis function, improves ETC activity and β -oxidation, and eventually attenuates lipid accumulation-induced hepatocyte injury by enhancing TG clearance. Due to limitations such as the animal model of NASH and lack of inhibitors or blockers in our current study, further research is needed to investigate the detailed molecular mechanisms and potential clinical applications of ACNs in NAFLD.

■ ASSOCIATED CONTENT

● Supporting Information

Composition of the purified anthocyanins and primer sequences used for RT-PCR. This material is available free of charge via the Internet at <http://pubs.acs.org>.

■ AUTHOR INFORMATION

Corresponding Authors

*Phone: 86-751-8120167. Fax: 86-751-8121429. E-mail: guohh1999@hotmail.com.

*Phone: 86-20-87331597. Fax: 86-20-87330446. E-mail: lingwh@mail.sysu.edu.cn.

Funding

This work was funded by grants from the National Basic Research Program (973 Program, 2012CB517506), National Nature Science Foundation (81172655, 81372994), and China Scholarship Council (201308440005).

Notes

The authors declare no competing financial interest.

■ ABBREVIATIONS USED

α -SMA, alpha smooth muscle actin; ACNs, anthocyanins; ALT, alanine aminotransferase; AMPK, AMP-activated protein kinase; AST, aspartate aminotransferase; complex I, nicotinamide adenine dinucleotide dehydrogenase; complex IV, cytochrome c oxidase; CPS-1, carbamoyl phosphate synthase 1; CPT-1, carnitine palmitoyltransferase 1; DHE, dihydroethidium; ETC, electron transfer chain; FAS, fatty acid synthesis; H&E, hematoxylin and eosin; HSC, hepatic stellate cell; MCAD, medium chain acyl CoA dehydrogenase; MCD, methionine-choline-deficient diet; MDA, malondialdehyde; MRC, mitochondrial respiratory chain; mtDNA, mitochondrial DNA; NAFLD, nonalcoholic fatty liver disease; NAS, nonalcoholic fatty liver disease activity scoring; NASH, nonalcoholic steatohepatitis; NRF-1/2, nuclear respiratory factor-1/2; p-AMPK, phosphorylated AMP-activated protein kinase; PGC-1 α/β , peroxisome proliferator-activated receptor- γ coac-

tivator-1 α/β ; PPAR- α , peroxisome proliferator-activated receptor- α ; ROS, reactive oxygen species; TC, total cholesterol; Tfam, transcription factor A; TG, triglyceride; VLDL, very low density lipoprotein-triglyceride

■ REFERENCES

- (1) Shen, H. C.; Zhao, Z. H.; Hu, Y. C.; Chen, Y. F.; Tung, T. H. Relationship between obesity, metabolic syndrome, and nonalcoholic fatty liver disease in the elderly agricultural and fishing population of Taiwan. *Clin. Interventions Aging* **2014**, *9*, 501–508.
- (2) Tiniakos, D. G.; Vos, M. B.; Brunt, E. M. Nonalcoholic fatty liver disease: pathology and pathogenesis. *Annu. Rev. Pathol.* **2010**, *5*, 145–171.
- (3) Caldwell, S. H.; Chang, C. Y.; Nakamoto, R. K.; Krugner-Higby, L. Mitochondria in nonalcoholic fatty liver disease. *Clin. Liver Dis.* **2004**, *8*, 595–617 x.
- (4) Sobaniec-Lotowska, M. E.; Lebensztejn, D. M. Ultrastructure of hepatocyte mitochondria in nonalcoholic steatohepatitis in pediatric patients: usefulness of electron microscopy in the diagnosis of the disease. *Am. J. Gastroenterol.* **2003**, *98*, 1664–1665.
- (5) Perez-Carreras, M.; Del Hoyo, P.; Martin, M. A.; Rubio, J. C.; Martin, A.; Castellano, G.; Colina, F.; Arenas, J.; Solis-Herruzo, J. A. Defective hepatic mitochondrial respiratory chain in patients with nonalcoholic steatohepatitis. *Hepatology* **2003**, *38*, 999–1007.
- (6) Finocchietto, P. V.; Holod, S.; Barreiro, F.; Peralta, J. G.; Alippe, Y.; Giovambattista, A.; Carreras, M. C.; Poderoso, J. J. Defective leptin-AMP-dependent kinase pathway induces nitric oxide release and contributes to mitochondrial dysfunction and obesity in ob/ob mice. *Antioxid. Redox Signaling* **2011**, *15*, 2395–2406.
- (7) Roglans, N.; Vila, L.; Farre, M.; Alegret, M.; Sanchez, R. M.; Vazquez-Carrera, M.; Laguna, J. C. Impairment of hepatic Stat-3 activation and reduction of PPAR α activity in fructose-fed rats. *Hepatology* **2007**, *45*, 778–788.
- (8) Serviddio, G.; Giudetti, A. M.; Bellanti, F.; Priore, P.; Rollo, T.; Tamborra, R.; Siculella, L.; Vendemiale, G.; Altomare, E.; Gnoni, G. V. Oxidation of hepatic carnitine palmitoyl transferase-I (CPT-I) impairs fatty acid β -oxidation in rats fed a methionine-choline deficient diet. *PLoS One* **2011**, *6*, e24084.
- (9) Kuo, J. J.; Chang, H. H.; Tsai, T. H.; Lee, T. Y. Positive effect of curcumin on inflammation and mitochondrial dysfunction in obese mice with liver steatosis. *Int. J. Mol. Med.* **2012**, *30*, 673–679.
- (10) Marcolin, E.; San-Miguel, B.; Vallejo, D.; Tieppo, J.; Marroni, N.; Gonzalez-Gallego, J.; Tunon, M. J. Quercetin treatment ameliorates inflammation and fibrosis in mice with nonalcoholic steatohepatitis. *J. Nutr.* **2012**, *142*, 1821–1828.
- (11) Shih, P. H.; Hwang, S. L.; Yeh, C. T.; Yen, G. C. Synergistic effect of cyanidin and PPAR agonist against nonalcoholic steatohepatitis-mediated oxidative stress-induced cytotoxicity through MAPK and Nrf2 transduction pathways. *J. Agric. Food Chem.* **2012**, *60*, 2924–2933.
- (12) Masterjohn, C.; Bruno, R. S. Therapeutic potential of green tea in nonalcoholic fatty liver disease. *Nutr. Rev.* **2012**, *70*, 41–56.
- (13) Liu, Y.; Wang, D.; Zhang, D.; Lv, Y.; Wei, Y.; Wu, W.; Zhou, F.; Tang, M.; Mao, T.; Li, M.; Ji, B. Inhibitory effect of blueberry polyphenolic compounds on oleic acid-induced hepatic steatosis in vitro. *J. Agric. Food Chem.* **2011**, *59*, 12254–12263.
- (14) Guo, H.; Liu, G.; Zhong, R.; Wang, Y.; Wang, D.; Xia, M. Cyanidin-3-O- β -glucoside regulates fatty acid metabolism via an AMP-activated protein kinase-dependent signaling pathway in human HepG2 cells. *Lipids Health Dis.* **2012**, *11*, 10.
- (15) Chang, J. J.; Hsu, M. J.; Huang, H. P.; Chung, D. J.; Chang, Y. C.; Wang, C. J. Mulberry anthocyanins inhibit oleic acid induced lipid accumulation by reduction of lipogenesis and promotion of hepatic lipid clearance. *J. Agric. Food Chem.* **2013**, *61*, 6069–6076.
- (16) Hwang, Y. P.; Choi, J. H.; Han, E. H.; Kim, H. G.; Wee, J. H.; Jung, K. O.; Jung, K. H.; Kwon, K. I.; Jeong, T. C.; Chung, Y. C.; Jeong, H. G. Purple sweet potato anthocyanins attenuate hepatic lipid accumulation through activating adenosine monophosphate-activated protein kinase

in human HepG2 cells and obese mice. *Nutr. Res. (N.Y.)* **2011**, *31*, 896–906.

(17) Cho, B. O.; Ryu, H. W.; Jin, C. H.; Choi, D. S.; Kang, S. Y.; Kim, D. S.; Byun, M. W.; Jeong, I. Y. Blackberry extract attenuates oxidative stress through up-regulation of Nrf2-dependent antioxidant enzymes in carbon tetrachloride-treated rats. *J. Agric. Food Chem.* **2011**, *59*, 11442–11448.

(18) Zhang, Z. F.; Lu, J.; Zheng, Y. L.; Wu, D. M.; Hu, B.; Shan, Q.; Cheng, W.; Li, M. Q.; Sun, Y. Y. Purple sweet potato color attenuates hepatic insulin resistance via blocking oxidative stress and endoplasmic reticulum stress in high-fat-diet-treated mice. *J. Nutr. Biochem.* **2013**, *24*, 1008–1018.

(19) Qin, Y.; Xia, M.; Ma, J.; Hao, Y.; Liu, J.; Mou, H.; Cao, L.; Ling, W. Anthocyanin supplementation improves serum LDL- and HDL-cholesterol concentrations associated with the inhibition of cholesteryl ester transfer protein in dyslipidemic subjects. *Am. J. Clin. Nutr.* **2009**, *90*, 485–492.

(20) Kleiner, D. E.; Brunt, E. M.; Van Natta, M.; Behling, C.; Contos, M. J.; Cummings, O. W.; Ferrell, L. D.; Liu, Y. C.; Torbenson, M. S.; Unalp-Arida, A.; Yeh, M.; McCullough, A. J.; Sanyal, A. J. Design and validation of a histological scoring system for nonalcoholic fatty liver disease. *Hepatology* **2005**, *41*, 1313–1321.

(21) Luo, X.; Xiao, Y.; Song, F.; Yang, Y.; Xia, M.; Ling, W. Increased plasma S-adenosyl-homocysteine levels induce the proliferation and migration of VSMCs through an oxidative stress-ERK1/2 pathway in apoE(–/–) mice. *Cardiovasc. Res.* **2012**, *95*, 241–250.

(22) Aoyama, T.; Hida, K.; Kuroda, S.; Seki, T.; Yano, S.; Shichinohe, H.; Iwasaki, Y. Edaravone (MCI-186) scavenges reactive oxygen species and ameliorates tissue damage in the murine spinal cord injury model. *Neurol. Med. Chir. (Tokyo)* **2008**, *48*, 539–545.

(23) Steinberg, G. R.; Kemp, B. E. AMPK in Health and Disease. *Physiol. Rev.* **2009**, *89*, 1025–1078.

(24) Hock, M. B.; Kralli, A. Transcriptional control of mitochondrial biogenesis and function. *Annu. Rev. Physiol.* **2009**, *71*, 177–203.

(25) Ruiz, L. M.; Jensen, E. L.; Bustos, R. I.; Arguello, G.; Gutierrez-Garcia, R.; Gonzalez, M.; Hernandez, C.; Paredes, R.; Simon, F.; Riedel, C.; Ferrick, D.; Elorza, A. A. Adaptive responses of mitochondria to mild copper deprivation involve changes in morphology, OXPHOS remodeling and bioenergetics. *J. Cell. Physiol.* **2014**, *229*, 607–619.

(26) Mandard, S.; Muller, M.; Kersten, S. Peroxisome proliferator-activated receptor alpha target genes. *Cell. Mol. Life Sci.* **2004**, *61*, 393–416.

(27) Guo, H.; Xia, M.; Zou, T.; Ling, W.; Zhong, R.; Zhang, W. Cyanidin 3-glucoside attenuates obesity-associated insulin resistance and hepatic steatosis in high-fat diet-fed and *db/db* mice via the transcription factor FoxO1. *J. Nutr. Biochem.* **2012**, *23*, 349–360.

(28) Begriche, K.; Massart, J.; Robin, M. A.; Bonnet, F.; Fromenty, B. Mitochondrial adaptations and dysfunctions in nonalcoholic fatty liver disease. *Hepatology* **2013**, *58*, 1497–1507.

(29) Begriche, K.; Massart, J.; Robin, M. A.; Borgne-Sanchez, A.; Fromenty, B. Drug-induced toxicity on mitochondria and lipid metabolism: mechanistic diversity and deleterious consequences for the liver. *J. Hepatol.* **2011**, *54*, 773–794.

(30) Rector, R. S.; Thyfault, J. P.; Uptergrove, G. M.; Morris, E. M.; Naples, S. P.; Borengasser, S. J.; Mikus, C. R.; Laye, M. J.; Laughlin, M. H.; Booth, F. W.; Ibdah, J. A. Mitochondrial dysfunction precedes insulin resistance and hepatic steatosis and contributes to the natural history of non-alcoholic fatty liver disease in an obese rodent model. *J. Hepatol.* **2010**, *52*, 727–736.

(31) Kubli, D. A.; Gustafsson, A. B. Mitochondria and mitophagy: the yin and yang of cell death control. *Circ. Res.* **2012**, *111*, 1208–1221.

(32) Anstee, Q. M.; Goldin, R. D. Mouse models in non-alcoholic fatty liver disease and steatohepatitis research. *Int. J. Exp. Pathol.* **2006**, *87*, 1–16.

(33) Lee, W. J.; Kim, M.; Park, H. S.; Kim, H. S.; Jeon, M. J.; Oh, K. S.; Koh, E. H.; Won, J. C.; Kim, M. S.; Oh, G. T.; Yoon, M.; Lee, K. U.; Park, J. Y. AMPK activation increases fatty acid oxidation in skeletal muscle by activating PPARalpha and PGC-1. *Biochem. Biophys. Res. Commun.* **2006**, *340*, 291–295.

(34) Scarpulla, R. C.; Vega, R. B.; Kelly, D. P. Transcriptional integration of mitochondrial biogenesis. *Trends. Endocrinol. Metab.* **2012**, *23*, 459–466.

(35) Jiang, X.; Tang, X.; Zhang, P.; Liu, G.; Guo, H. Cyanidin-3-O-beta-glucoside protects primary mouse hepatocytes against high glucose-induced apoptosis by modulating mitochondrial dysfunction and the PI3K/Akt pathway. *Biochem. Pharmacol.* **2014**, *90*, 135–144.

(36) Lee, S. J.; Zhang, J.; Choi, A. M.; Kim, H. P. Mitochondrial dysfunction induces formation of lipid droplets as a generalized response to stress. *Oxid. Med. Cell. Longevity* **2013**, *2013*, 327167.